

**Partial, total, and resonance production cross sections for the reactions
 $\pi^+p \rightarrow$ four-prong final states at 10.3 GeV/c**

C. N. Kennedy,* P. D. Zemany,[†] J. Beaufays, A. W. Key, G. J. Luste, J. D. Prentice, and T.-S. Yoon

Department of Physics, University of Toronto, Toronto, Ontario M5S 1A7, Canada

(Received 18 July 1977)

The major production channels of four-prong final states resulting from π^+p interactions at a center-of-mass energy of 4.5 GeV are studied. In addition to total production cross sections, comprehensive listings of partial and resonance production cross sections are also given for each final state of interest. All final states, including $n\pi^+\pi^+\pi^+\pi^-$, are found to exhibit copious resonance production.

I. INTRODUCTION

A. Experimental procedure

The data reported herein come from an 8.5-events/ μ b exposure of the SLAC 82-in. hydrogen bubble chamber to a 10.3-GeV/c π^+ beam. Ninety percent of the resulting four-prong final states were measured on Toronto's automatic measuring machine, POLLY III, while the remaining 10% were measured on conventional manual machines as a check against possible POLLY measuring biases. No discernible biases were observed. All events were processed through the BRAVE-TVGP-SQUAW sequence of programmes which reconstructed and fitted them to specified final states. We considered all channels for which we expected detectable cross sections at our level of statistical accuracy. The seven reactions fitted for were

- $\pi^+p \rightarrow \pi^+p\pi^+\pi^-$ (9983 events) } (1)
- $\pi^+p \rightarrow \pi^+pK^+K^-$ (552 events) } 4C (2)
- $\pi^+p \rightarrow \pi^+pp\bar{p}$ (122 events) } (3)
- $\pi^+p \rightarrow \pi^+p\pi^+\pi^-\pi^0$ (10 428 events) } (4)
- $\pi^+p \rightarrow n\pi^+\pi^+\pi^+\pi^-$ (3088 events) } 1C (5)
- $\pi^+p \rightarrow \pi^+p\pi^+\pi^-$ MM (24 039 events) } (6)
- $\pi^+p \rightarrow \pi^+\pi^+\pi^+\pi^-$ MM (10 107 events) } 0C (7)

After an event has been processed through SQUAW it is then ready for the next step in the data processing chain, the Toronto automatic hypothesis-selection program FRED A. Here one of three things will happen. Either (a) the measurement will be deemed unsatisfactory and the event returned for a remeasure, or (b) FRED A will be unable to decide on a unique hypothesis for the event and it will be sent for manual editing, or (c) FRED A will successfully use its fit-selection algorithm¹ to decide on a unique hypothesis assignment for the event and it will then be added

to our data-summary tape (DST). Events in categories (a) and (b) above were also eventually added to our DST after being assigned a unique hypothesis. A comprehensive description of all experimental and data-reduction procedures (beam-path-length calculation, normalization, scanning and measuring, hypothesis selection, contamination and loss estimation, etc.) can be found elsewhere.^{2,3}

B. Production cross sections

Taking into account scanning and measuring efficiencies, contaminations, losses, and fiducial-volume corrections, we have calculated production cross sections for reactions (1)-(7) at 10.3-GeV/c incident pion momentum. These measured cross sections are presented in Table I where they are compared with those from previous experiments. In addition, our contamination estimate for each reaction data sample is also given.

In Sec. II we discuss the procedures used to fit the observed resonances and present the partial and resonance production cross sections for each of the seven reactions studied. Invariant-mass plots for all particle combinations in each reaction are also displayed. Finally, a brief summary of our findings is given in Sec. III.

II. PARTIAL AND RESONANCE PRODUCTION CROSS SECTIONS

At 4.5-GeV center-of-mass energy, the reactions $\pi^+p \rightarrow$ four-prong final states are rich in baryon- and meson-resonance production. In this section we shall display those invariant-mass distributions for each particle combination which exhibits resonance production in each of the seven reactions studied. In general, we used a combination of background (either phase space or phase space multiplied by a polynomial in mass) and one or more Breit-Wagner functions multiplied by background to fit the invariant-mass distributions of interest and thus calculate the partial and reso-

TABLE I. Production cross sections for the reactions $\pi^+p \rightarrow$ four-prong final states at 10.3 GeV/c.

Final state	Contamination (%)	Cross section (μb)	
		Predicted ^a	Measured
(1) $\pi^+p\pi^+\pi^-$	2.3 ± 0.6	$1\ 640 \pm 60$	$1\ 648 \pm 120$
(2) $\pi^+pK^+K^-$	< 4	84 ± 28	86 ± 7
(3) $\pi^+p\rho\bar{\rho}$	< 3	16 ± 2	18.8 ± 2.2
(4) $\pi^+p\pi^+\pi^-\pi^0$	16.4 ± 1.2^b	$1\ 622 \pm 79$	$1\ 654 \pm 120$
(5) $n\pi^+\pi^+\pi^-\pi^-$	2.9 ± 1.7	568 ± 30	503 ± 38
(6) $\pi^+p\pi^+\pi^-MM$	c	d	$4\ 465^e$
(7) $\pi^+\pi^+\pi^+\pi^-MM$	c	d	$1\ 880^e$
Missing mass ^f	3.6 ± 0.7	d	$6\ 345 \pm 455$
Four prongs	c	$9\ 650 \pm 120^g$	$10\ 390 \pm 750$

^a Obtained by fitting the existing data above 4 GeV/c to the function $\sigma = kP_{\text{lab}}^n$.

^b Deleting events with $MM^2 > (2m_{\pi^0})^2$ reduces this contamination to $(5.6 \pm 1.1)\%$.

^c No estimate attempted.

^d Data too scanty to fit.

^e Obtained by considering the missing-mass cross section and the ratio of the reaction (6) to reaction (7) candidates. No error estimate has been attempted.

^f Reactions (6) and (7) together.

^g Measurement at 8.04 GeV/c. The total four-prong production cross section does not exhibit the functional form quoted in footnote a.

nance production cross sections for each final state.⁴ Estimates of contamination from, and losses to, other channels as well as corrections for the resonance tails were taken into account in these calculations. The mass and full width of the resonance were constrained within the limits quoted by the Particle Data Group.⁵ The quoted errors for the number of resonant events include the effects of correlations between the fitted parameters. Any specific deviations from the above procedure are discussed in Secs. IIA–IIE below.

A. The reaction $\pi^+p \rightarrow \pi^+p\pi^+\pi^-$

As can be seen in Figs. 1 and 2, the reaction $\pi^+p \rightarrow \pi^+p\pi^+\pi^-$ exhibits copious baryon- and meson-resonance production at 10.3-GeV/c incident pion momentum. A comparison of Figs. 1(a) and 1(b) indicates that Δ^{++} production is predominantly associated with the slower of the two produced π^+ 's (in the laboratory frame of reference) (the slower and faster pions are henceforth designated by π_s^+ and π_f^+ , respectively). In addition to the

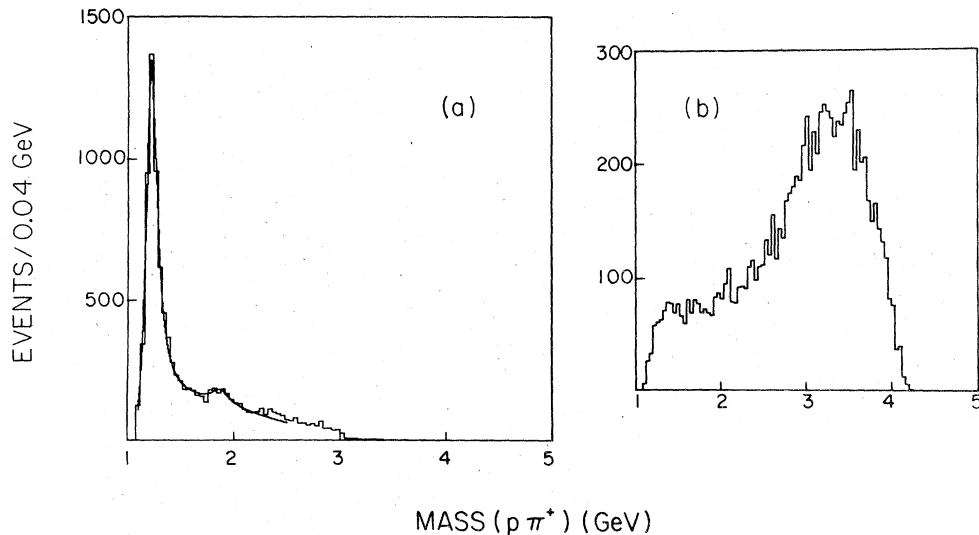


FIG. 1. The $p\pi^+$ invariant-mass distributions for reaction (1). (a) The $p\pi_s^+$ distribution. The solid curve represents our fit to the data as described in the text. (b) The $p\pi_f^+$ distribution.

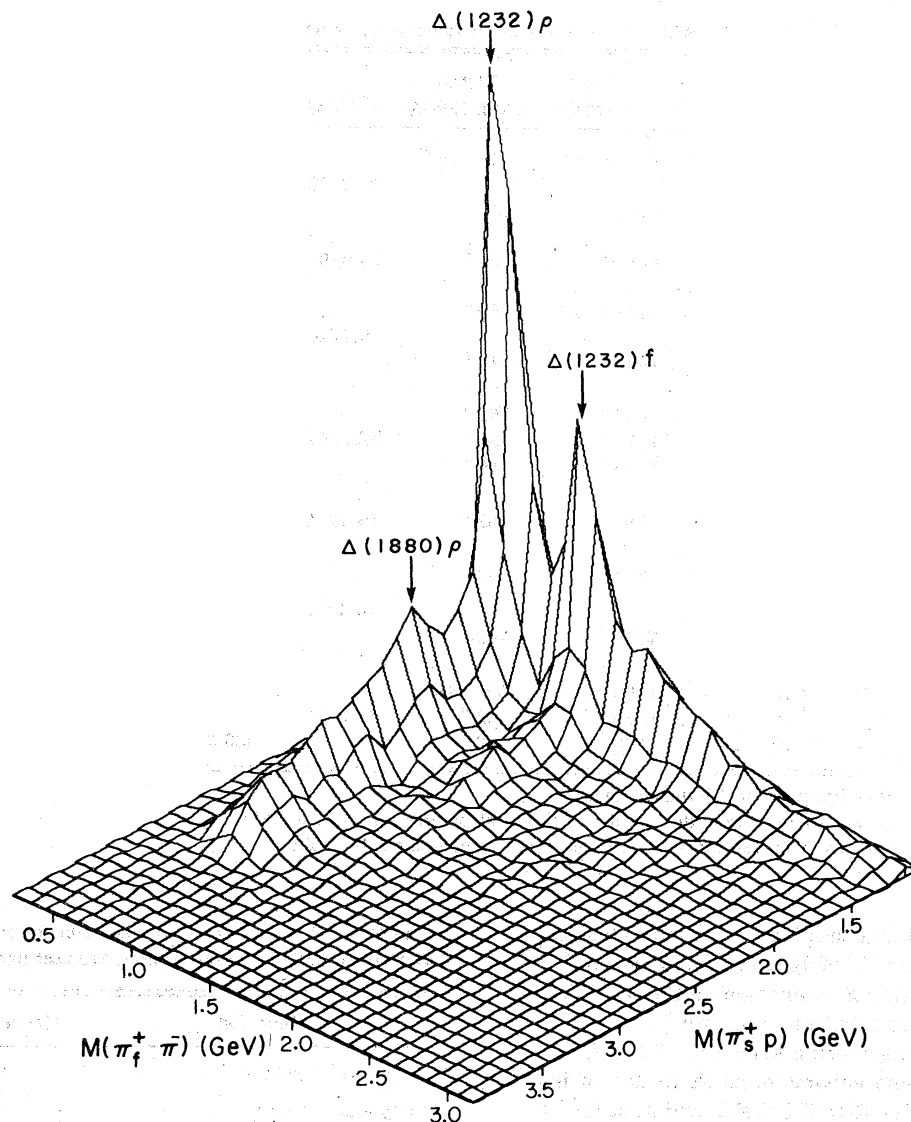


FIG. 2. $\pi_f^+ \pi^-$ invariant mass vs $p \pi_s^+$ invariant mass for reaction (1). The peaks are a reflection of quasi-two-body production.

striking $\Delta^{++}(1232)$ signal seen in the $p \pi_s^+$ distribution there is also a $\Delta^{++}(1880)$ signal clearly present.⁶ The quantitative results of our fit to the $p \pi_s^+$ distribution are given in Table II. A fit to the $p \pi_f^+$ distribution indicated that, within error, no Δ^{++} events were present.

Production of the Δ resonance is often accompanied by ρ - or f -meson production. The presence of these quasi-two-body states can be seen in Fig. 2 which shows clear ρ , f , and Δ bands, the regions where the bands intersect showing enhancements due to quasi-two-body production.

To determine the $\Delta \rho$ and Δf production cross sections a two-dimensional fit to the data must be

made. This was done using a slice technique⁷ in which the number of Δ 's in several $\pi_f^+ \pi^-$ invariant-mass slices were determined by fitting. The resulting $\pi_f^+ \pi^-$ invariant-mass distribution of these Δ events was then fitted to determine the number of ρ 's and f 's in the signal above background. Details of this procedure for the $\Delta(1232)$ and the $\Delta(1880)$ are given by Zemany *et al.*⁸ The production cross sections for the quasi-two-body states $\Delta \rho$ and Δf are listed in Table III.

Inspection of the $\pi^+ \pi^-$ invariant-mass distributions [Figs. 3(a)–(3c)] reveals production of the $\rho(770)$ and $f(1270)$ mesons, and a statistically insignificant bump at the location of the $g(1680)$.⁴

TABLE II. Resonance production in reaction (1).

Particle combination	Resonance	Fitted mass (MeV)	Fitted width (MeV)	χ^2/NDF	Number of fitted events	Cross section (μb)
$p\pi_s^+$	$\Delta^{++}(1232)$	1220 ± 5^b	90 ± 10^b	33.3/33	5464 ± 131	902 ± 69
	$\Delta^{++}(1880)$	1871^a	205^a		382 ± 60	63 ± 11
$p\pi^-$	$\Delta^0(1232)$	1213^a	95^a	12.8/9	403 ± 67	67 ± 12
$p\pi_s^+\pi^-$	$N(1470)$	1454 ± 20^b	180^a	19.7/14	707 ± 102	117 ± 19
	$N(1688)$	1688^a	140^a		566 ± 120	93 ± 21
$\pi_f^+\pi^-$	ρ	765^a	152^a	61.1/44	4392 ± 97	725 ± 55
	f	1270^a	180^a		1050 ± 80	173 ± 18
	g	1690^a	180^a		108 ± 70	18 ± 12
$\pi_s^+\pi^-$	ρ	765^a	152^a	19.7/16	1923 ± 102	317 ± 29
$\pi^+\pi^-$ (2/event)	ρ	765^a	152^a	36.5/31	5926 ± 146	978 ± 75
	f	1270^a	180^a		1790 ± 96	295 ± 27
$\pi^+\pi^+\pi^-$	A_1	1100^a	397 ± 49	21.3/33	1945 ± 115^c	321 ± 19^c
	A_2	1310^a	102^a		175 ± 42^c	29 ± 7^c
	A_3	1640^a	300^a		333 ± 79^c	55 ± 13^c

^a Value fixed in the fitting program.

^b Allowed to vary in order to obtain the best possible fit to the data.

^c Obtained from the spin-parity analysis discussed in Sec. II A.

The $p\pi_s^+\pi^-$ combination [Fig. 3(d)] indicates possible $N(1470)$ and $N(1670)$ baryon production,⁴ and a $\Delta^0(1232)$ signal is present in the $p\pi^-$ invariant-mass distribution [Fig. 3(e)].

The $\pi^+\pi^+\pi^-$ distribution shown in Fig. 3(f) shows a low-mass enhancement at values of invariant mass less than 1.5 GeV, and another at around 1.65 GeV. In order to separate the A mesons responsible for these enhancements and to quote reliable production cross sections we have carried out a simplified spin-parity analysis using a method similar to that of Lamsa *et al.*⁹ It was assumed that the A mesons decayed in a two-step process, and that the intermediate $\pi^+\pi^-$ system was an ϵ^0 meson (mass 0.70 GeV, width 0.30 GeV), a ρ^0 meson, or an f^0 meson. The following spin-parity states (J^P, l) were considered: 1^+S and 2^-P for the $\pi\rho$ system, 0^+S and 1^+P for the $\pi\epsilon$ system, and 2^+S for the πf system. A maximum-likelihood fit was performed in 100-MeV bins of the 3π mass distribution from which events containing the $\Delta^{++}(1232)$ [$m(p\pi^+) > 1.34$ GeV] were excluded. The results are shown in Fig. 4. The low-mass region is dominated by the 1^+ state (identified as the A_1 meson) and the higher-mass region by a 2^- state (the A_3 , centered at 1.6 GeV, with a width

TABLE III. Partial cross sections for reaction (1). The subscript nr refers to nonresonant production.

Reaction	Cross section (μb)
$\pi^+p \rightarrow \Delta^{++}(1232)\rho$	339 ± 37
$\pi^+p \rightarrow \Delta^{++}(1232)f$	174 ± 20
$\pi^+p \rightarrow \Delta^{++}(1232)g$	18 ± 12^a
$\pi^+p \rightarrow \Delta^{++}(1880)\rho$	31 ± 8
$\pi^+p \rightarrow \Delta^{++}(1880)f$	7 ± 4
$\pi^+p \rightarrow \Delta^{++}(1232)(\pi^+\pi^-)_{\text{nr}}$	371 ± 82
$\pi^+p \rightarrow \Delta^{++}(1880)(\pi^+\pi^-)_{\text{nr}}$	25 ± 14
$\pi^+p \rightarrow \Delta^0(1232)\pi^+\pi^+$	67 ± 12
$\pi^+p \rightarrow (\pi^+p)_{\text{nr}}\rho$	608 ± 84
$\pi^+p \rightarrow (\pi^+p)_{\text{nr}}f$	114 ± 34
$\pi^+p \rightarrow A_2^+p$	29 ± 7
$\pi^+p \rightarrow \pi^+N^+(1470)$	117 ± 19
$\pi^+p \rightarrow \pi^+N^+(1688)$	93 ± 21
Sum of partial cross section	1993 ± 135
Total production cross section	1648 ± 120

^a Upper limit.

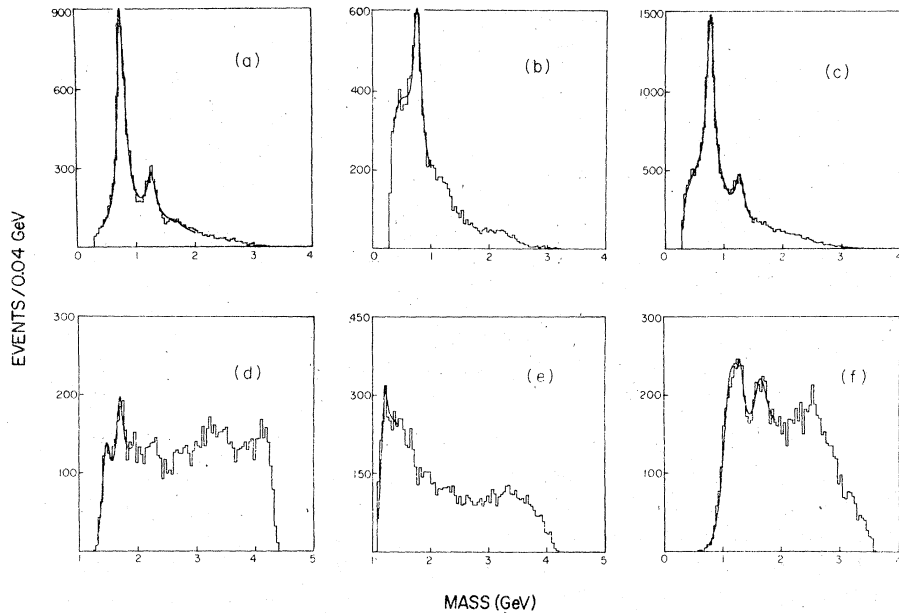


FIG. 3. Fitted reaction (1) invariant-mass distributions. The solid curves represent our fits to the data as described in the text. (a) $\pi_f^+ \pi^-$ (b) $\pi_s^+ \pi^-$ (c) $\pi^+ \pi^-$ (2 combinations/event) (d) $p \pi_s^+ \pi^-$ (e) $p \pi^-$ (f) $\pi^+ \pi^+ \pi^-$.

of 0.3 GeV) decaying to S -wave $f\pi$ ($\sim 65\%$) and P -wave $\rho\pi$ ($\sim 35\%$). The A_2 is seen as a distinct 2^+ peak at around 1.3 GeV.

The remaining invariant-mass distributions for this channel ($p\pi_f^+\pi_s^+$, $p\pi_f^+\pi^-$, $\pi_f^+\pi_s^+$) exhibit no resonant production.

The quantitative results of the above fits are given in Table II and the partial cross sections obtained from them are listed in Table III. An examination of Table III indicates that our reaction (1) data are consistent with 100% production via quasi- n -body intermediate states.

B. The reactions $\pi^+ p \rightarrow \pi^+ p K^+ K^-$ and $\pi^+ p \rightarrow \pi^+ p \bar{p}\bar{p}$

Figures 5(a)–5(c) display the $\pi^+ p$, $\pi^+ K^-$, and $K^+ K^-$ invariant-mass distributions, respectively, of reaction (2). A very strong $\Delta^{++}(1232)$ signal is evident in the $\pi^+ p$ distribution while an equally strong $K^*(892)$ signal can be seen in the $\pi^+ K^-$ distribution along with a smaller $K^*(1420)$ signal. Both these distributions were fitted as described in Sec. I to obtain the production cross sections of these three resonances. The $K\bar{K}$ distribution shown in Fig. 5(c) indicates the presence of $\phi(1020)$, $f(1270)$,¹⁰ and a narrow enhancement around 1580 MeV which we shall refer to as the “1580” (most likely a statistical fluctuation at the $2\frac{1}{2}$ standard deviation level). The latter two enhancements were fitted as described in Sec. I while for the $\phi(1020)$, we simply counted the number of events above a handdrawn background.¹¹

The results of the above fits are listed in Table IV and the partial cross sections obtained from them are given in Table V. Within error, the ϕ , f , and “1580” were found to be completely anti-

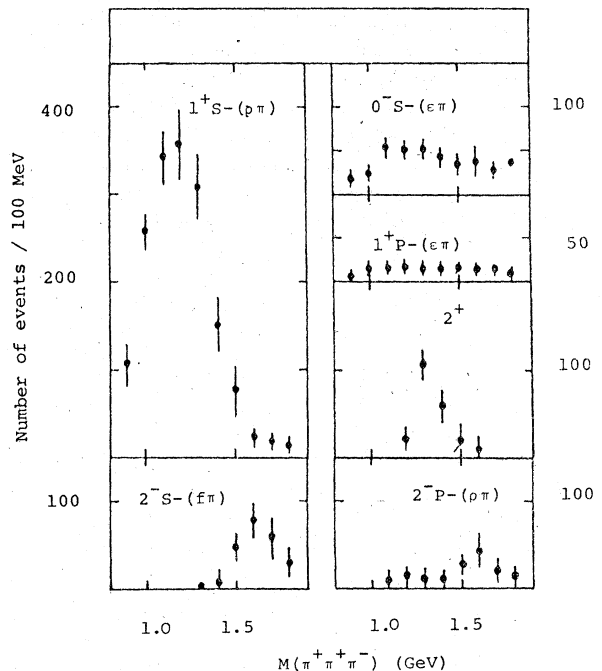


FIG. 4. Number of events in each spin-parity state (J^P, I) included in the fit to the 3π invariant-mass distributions of reaction (1).

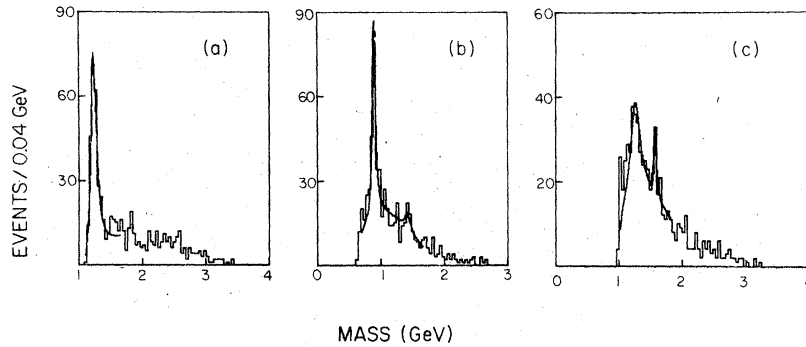


FIG. 5. Fitted reaction (2) invariant-mass distributions. The solid curves represent our fits to the data as described in the text. (a) $p\pi^+$ (b) π^+K^- (c) K^+K^- .

associated with the $\Delta^{++}(1232)$. As with reaction (1), reaction (2) is consistent with 100% production via quasi- n -body intermediate states.

The $\Delta^{++}(1232)$ is the only clear resonant state produced in reaction (3). This final state has been extensively discussed in a previous publication¹² to which the reader is referred for details.

C. The reaction $\pi^+p \rightarrow \pi^+p\pi^+\pi^-\pi^0$

The invariant-mass plots for those particle combinations in the $\pi^+p\pi^+\pi^-\pi^0$ final state which exhibit resonance behavior are displayed in Figs. 6 and 7. The quantitative results of the fits to these distributions are listed in Table VI.

As in reaction (1) there are distinct differences between distributions containing the π_s^+ and those containing the π_f^+ , the most striking contrast being apparent in the $p\pi_s^+$ and $p\pi_f^+$ invariant-mass distributions. With respect to these differences we have fitted certain invariant-mass distributions both with the fast and slow π^+ 's separately and together. This allows a consistency check on the cross-section

measurement as well as distinguishing between the different production mechanisms for the resonance in question. No other cuts have been used in the data with the exception of the 4π mass distribution. There we have used cuts in the 3π ($\pi^+\pi^-\pi^0$; 2 combinations/event) mass requiring either ω or η production¹³ to distinguish B^- and A_2^- -meson production, respectively. The relevant distributions are shown in Fig. 7. A listing of the partial cross sections for reaction (4) is given in Table VII.

D. The reaction $\pi^+p \rightarrow n\pi^+\pi^+\pi^-\pi^0$

At 4.5-GeV center-of-mass energy the final state $n\pi^+\pi^+\pi^-\pi^0$ is also rich in baryon- and meson-resonance production. These include $\Delta^{++}(1232)$, $\Delta^-(1232)$, $\Delta^{++}(1880)$, $N(1535)$, $\rho(770)$, $f(1270)$, and $A_2(1310)$, all of which are produced in measurable quantities. However, before we can calculate their production cross sections by fitting their invariant-mass distributions to Breit-Wigner functions we must first determine the functional form of the nonresonant background under them.

TABLE IV. Resonance production in reactions (2) and (3).

Reaction	Particle combination	Resonance	Fitted mass (MeV)	Fitted width (MeV)	χ^2/NDF	Number of fitted events	Cross section (μb)
(2)	$p\pi^+$	$\Delta^{++}(1232)$	1255 ± 4^a	99 ± 14^a	26.7/16	216 ± 20	34 ± 4
(2)	π^+K^-	$K^*(892)$	892^b	50^b	31.0/25	143 ± 19	22 ± 4
		$K^*(1420)$	1421^b	108^b		25 ± 10	3.9 ± 1.6
(2)	K^+K^-	ϕ	21.5/20	15 ± 5	2.3 ± 0.8
		f	1270^b	180^b		131 ± 19	20 ± 3
		"1580"	1580^b	40^b		27 ± 11	4.2 ± 1.7
(3)	$p_s\pi^+$	$\Delta^{++}(1232)$	1209 ± 10^a	132 ± 25^a	9.1/13	57 ± 10	8.8 ± 1.9

^a Allowed to vary in order to obtain the best possible fit to the data.

^b Value fixed in the fitting program.

TABLE V. Partial cross sections for reactions (2) and (3).

Reaction	Cross section (μb)
Reaction (2)	
$\pi^+p \rightarrow \pi^+p\phi$	2.3 ± 0.8
$\pi^+p \rightarrow \pi^+pf$	20 ± 3
$\pi^+p \rightarrow \pi^+p''(1580)$	4.2 ± 1.7
$\pi^+p \rightarrow \Delta^{++}(1232)K^+K^-$	34 ± 4
$\pi^+p \rightarrow \rho K^+K^*(892)$	22 ± 4
$\pi^+p \rightarrow \rho K^+K^*(1420)$	3.9 ± 1.6
Sum of partial cross sections	86 ± 7
Total production cross section	86 ± 7
Reaction (3)	
$\pi^+p \rightarrow \Delta^{++}(1232)p\bar{p}$	8.8 ± 1.9

1. Generating the nonresonant background

In order to determine this functional form we used the Monte Carlo event generation program SAGE¹⁴ to generate a large number of peripheral phase-space events. SAGE generated final-state particle four-vectors with a phase-space density corresponding to $\exp(-\sum_{i=1}^n p_i/2r)$ where p_i is the component of the i th outgoing particle's momentum transverse to the beam direction, and r is a parameter that characterizes the degree to which these components are limited in the generation. N is the number of final-state particles to be generated, five in our case.

A parameter that characterizes the limitation of transverse momenta and represents $\langle p_i^2 \rangle^{1/2}$ for the generated particles was also used. This

TABLE VI. Resonance production in reaction (4).

Particle combination	Resonance	Fitted mass (MeV)	Fitted width (MeV)	χ^2/NDF	Number of fitted events	Cross section (μb)
$p\pi_s^+$	$\Delta^{++}(1232)$	1208 ± 9^a	130 ± 12^a	42.0/26	4536 ± 180	809 ± 32
	$\Delta^{++}(1880)$	1871^b	205^b		220 ± 30	40 ± 5
$\pi_f^+\pi^0$	ρ^+	758 ± 10^a	120 ± 18^a	25.8/16	736 ± 65	132 ± 16
$\pi_f^+\pi^-$	ρ^0	757 ± 10^a	115 ± 19^a	42.1/28	1192 ± 110	203 ± 26
	f^0	1270^b	180^b		224 ± 48	40 ± 10
$\pi_s^+\pi^0$	ρ^+	726 ± 26^a	203 ± 50^a	12.5/13	1435 ± 90	256 ± 25
$\pi_s^+\pi^-$	ρ^0	770^b	152^b	13.1/17	754 ± 45	129 ± 14
$\pi^-\pi^0$	ρ^-	770 ± 6^a	165 ± 12^a	8.1/10	698 ± 65	124 ± 16
$\pi^+\pi^+\pi^-$	$A_2(1310)$	1310^b	102^b	9.7/14	301 ± 41	54 ± 9
	$F_1(1540)$	1540^b	60^b		68 ± 25	12 ± 5
$\pi_f^+\pi^-\pi^0$	$A_2(1310)$	1310^b	102^b	15.2/10	433 ± 39	77 ± 10
	$A_3(1640)$	1640^b	300^b		588 ± 46	105 ± 12
$\pi^+\pi^-$ (2/event)	ρ^0	760 ± 10^a	131 ± 20^a	47.6/20	2212 ± 110	378 ± 35
	f^0	1270^b	180^b		596 ± 100	106 ± 20
$\pi^+\pi^0$ (2/event)	ρ^+	765^b	152^b	18.7/14	1763 ± 142	314 ± 35
$\pi^+\pi^-\pi^0$ (2/event)	ω	783 ± 5^a	23.1 ± 5^a	62.0/55	691 ± 35	123 ± 12
	η	551 ± 4^a	12.5 ± 4^a		101 ± 13	18 ± 3
$\pi^+\pi^+\pi^-\pi^0$	$B \rightarrow \omega\pi^+$	1201 ± 15^a	125^b	28.2/22	101 ± 20	18 ± 4
	$g \rightarrow (4\pi)^+$	1690^b	180^b	21.2/18	277 ± 60	50 ± 11
	$A_2 \rightarrow \eta\pi^+$	1310^b	102^b	15.3/21	31 ± 9	5.5 ± 2

^a Allowed to vary in order to obtain the best possible fit to the data.^b Value fixed in the fitting program.

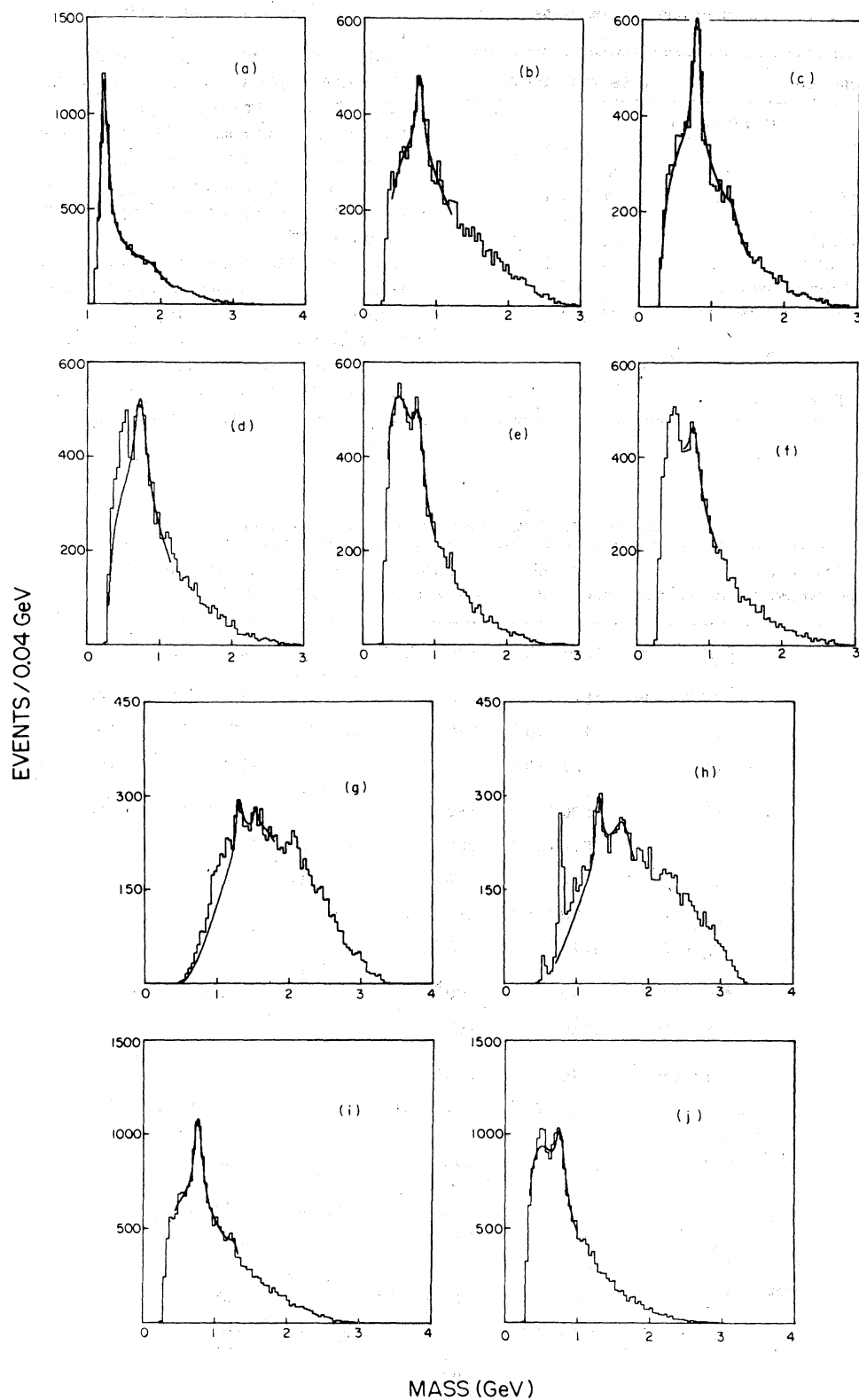


FIG. 6. Fitted reaction (4) invariant-mass distributions. The solid curves represent our fits to the data as described in the text. (a) $p\pi_s^+$ (b) $\pi_s^+\pi^0$ (c) $\pi_s^+\pi^-$ (d) $\pi_s^+\pi^0$ (e) $\pi_s^+\pi^-$ (f) $\pi^-\pi^0$ (g) $\pi^+\pi^+\pi^-$ (h) $\pi_s^+\pi^-\pi^0$ (i) $\pi^+\pi^-$ (2 combinations/event) (j) $\pi^+\pi^0$ (2 combinations/event).

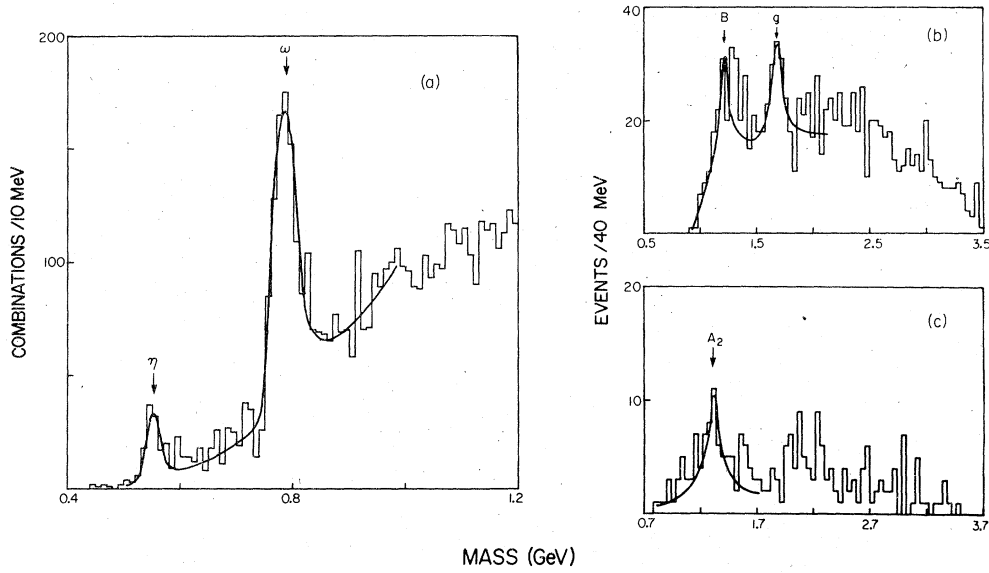


FIG. 7. Fitted invariant-mass distributions for reaction (4). (a) $\pi^+ \pi^- \pi^0$ (2 combinations/event) (b) $\pi^+ \pi^+ \pi^- \pi^0$ for events satisfying the ω mass cut described in the text. (c) $\pi^+ \pi^+ \pi^- \pi^0$ for events satisfying the η mass cut described in the text.

parameter R determines the distribution of the transverse momenta of the generated particles and is related to the standard deviation of the Gaussian distribution by

$$R = \langle p_t^2 \rangle^{1/2} = 2r^2(N-1)/N. \quad (8)$$

We set $R=0.4$ GeV/ c since this is what has been found experimentally in the past. As hoped for,

TABLE VII. Partial cross sections for reaction (4). The subscript nr refers to nonresonant production.

Reaction	Cross section (μb)
$\pi^+ p \rightarrow \Delta^{++}(1232)(\pi^+ \pi^- \pi^0)_{\text{nr}}$	752 ± 32
$\pi^+ p \rightarrow \Delta^{++}(1232)\omega$	45 ± 5
$\pi^+ p \rightarrow \Delta^{++}(1880)(\pi^+ \pi^- \pi^0)_{\text{nr}}$	24 ± 6
$\pi^+ p \rightarrow \Delta^{++}(1880)\omega$	16 ± 3
$\pi^+ p \rightarrow \pi^+ p \rho^+ \pi^-$	256 ± 25^a
$\pi^+ p \rightarrow \pi^+ p \rho^0 \pi^0$	129 ± 14^a
$\pi^+ p \rightarrow (\pi^+ p)_{\text{nr}} \omega$	44 ± 13^b
$\pi^+ p \rightarrow (\pi^+ p)_{\text{nr}} \eta$	12 ± 4
$\pi^+ p \rightarrow p F_1(1540)\pi^0$	12 ± 5
$\pi^+ p \rightarrow B^+(1235)p$	18 ± 4
Sum of partial cross sections	1308 ± 46
Total production cross section	1654 ± 120

^a Lower limit.

^b No B meson.

this value of R proved very satisfactory and no further adjustment to this parameter was required.

Using this peripheral phase-space background the invariant-mass distributions of interest were then fitted as described in Sec. II.

2. Resonance production cross sections

In Figs. 8(a)–8(d) we display the $n\pi^-$, $n\pi^+$, $n\pi^+\pi^+$, and $\pi^+\pi^-$ invariant-mass distributions for the 3088 neutron events in our final physics data sample. The curves superimposed on these distributions represent our overall fits to the data.

The $\Delta^+(1232)$, the $\rho(770)$, and the $f(1270)$ dominate the resonance production in this channel with some indication of the resonances $\Delta^+(1232)$, $N(1535)$, $\Delta^{++}(1880)$, and $A_2(1310)$. The cross sections depend on the precise nature of the assumed background. The accumulation of events in the $n\pi^+$ distribution at the $\Delta^+(1232)$ and $N(1535)$ is enhanced by the exclusion of combinations which include the fastest π^+ [Fig. 8(b), shaded histogram]. A fit to the $n\pi^+$ invariant-mass distribution to two Breit-Wigner shapes and the Monte Carlo-generated background indicates that we cannot demonstrate the production of these resonances at a statistically significant level. However, the values of cross sections so determined are quoted for the sake of completeness.⁴

The presence of an enhancement above the Monte Carlo background in the $(n\pi^+ \pi_s^+)$ mass distribution in the region of 1.9 GeV is also apparent⁶; details of the enhancement in this and other final

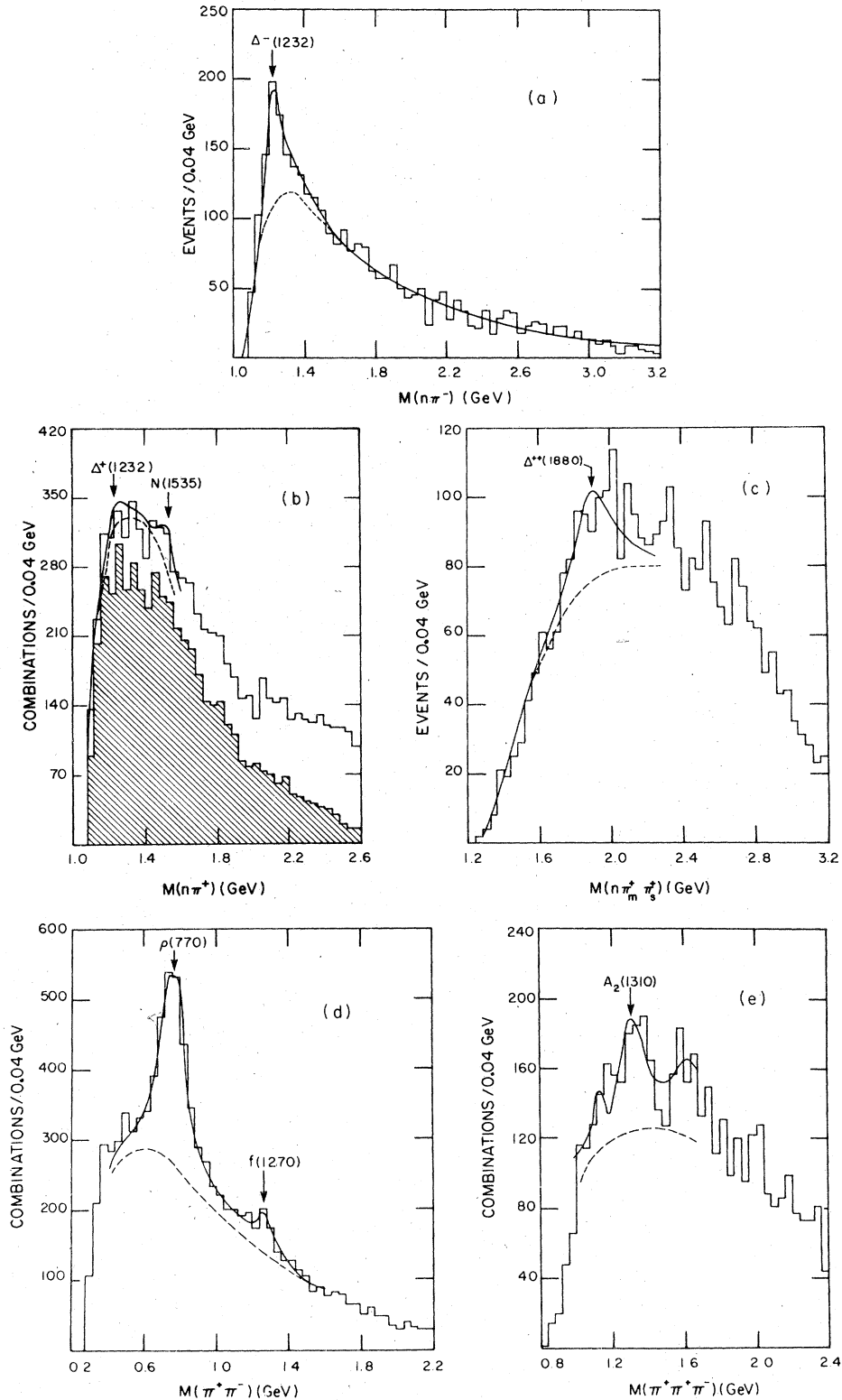


FIG. 8. Fitted reaction (5) invariant-mass distributions. The solid curves represent our fits to the data as described in the text. (a) $n\pi^-$ (b) $n\pi^+$ (in the shaded histogram, combinations which include the fastest π^+ are excluded) (c) $n\pi_m^+\pi_s^+$ (fastest π^+ in laboratory frame of references excluded); (d) $\pi^+\pi^-$ (3 combinations/event); (e) $\pi^+\pi^+\pi^-$ (only combinations which had at least one of their $\pi^+\pi^-$ combinations in the ρ mass band have been plotted).

TABLE VIII. Resonance production in reaction (5).

Resonance produced	Number of fitted events	χ^2/NDF	Fitted mass (MeV)	Fitted width (MeV)	Percentage ^a of total sample	Cross section ^a (μb)
$\rho(770)$	1559 ± 65	15.9/25	770	155	52	261 ± 23
$\Delta^-(1232)$	324 ± 20	93.1/69	1230	120	11	54 ± 5
$f(1270)$	269 ± 25	15.9/25	1266	160	9	45 ± 5
$A_2(1310)$	184 ± 20	23.4/13	1315	107	8	39 ± 5
$\Delta^{++}(1880)$	213 ± 50	25.5/22	1893 ± 25^b	244 ± 45^b	7	36 ± 9
$N(1535)$	157 ± 60	11.6/8	1525	74	5	26 ± 10
$\Delta^+(1232)$	54 ± 22	11.6/8	1230	120	2	9 ± 4

^a These numbers have been adjusted to take into account both the losses and contaminations inherent in the neutron data sample.

^b The mass and full width of the $\Delta^{++}(1880)$ were allowed to vary in order to obtain the best possible fit to the data.

states are provided in Ref. 8.

To investigate A_2 production we plotted every $\pi^+\pi^+\pi^-$ invariant-mass combination which had at least one of the $\pi^+\pi^-$ combinations in the ρ mass band [$0.62 \text{ GeV} < m(\pi^+\pi^-) < 0.94 \text{ GeV}$] since it is well known that the 3π decay of the A_2 goes 100% via $\rho\pi$.⁵ This distribution was then fitted to a Breit-Wigner function for the A_2 , two Breit-Wigner functions for the A_1 and A_3 kinematic enhancements, and a polynomial for the background. The qualitative results of this fit are displayed in Fig. 8(e).

The quantitative results of all the above fits are given in Table VIII where the resonance production cross sections, adjusted for both contaminations and losses, are quoted. For the A_2 cross section, corrections for the ρ tails have also been taken in-

to account.

The remaining two-, three-, and four-body invariant-mass distributions exhibit no significant enhancements above the smooth background. It should be noted that the amount of resonance formation present in this final state depends on the precise nature of the assumed background. The Monte Carlo calculation described above does seem to give a good representation of this background, and it would be difficult to believe that the resonances reported in Table VIII are not indeed present in this final channel, with the possible exception of the $N(1535)$ and the $\Delta(1232)$. However, even excluding these enhancements from consideration, it is clear that at least 80% of reaction (5) can be attributed to intermediate reso-

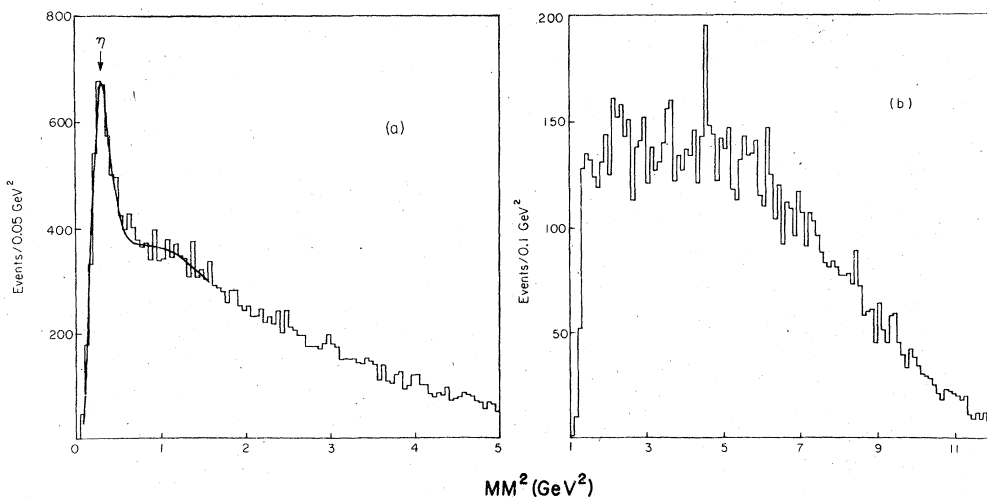


FIG. 9. Missing-mass-squared distributions. (a) Reaction (6). The solid curve represents our fit to the data as described in the text. (b) Reaction (7).

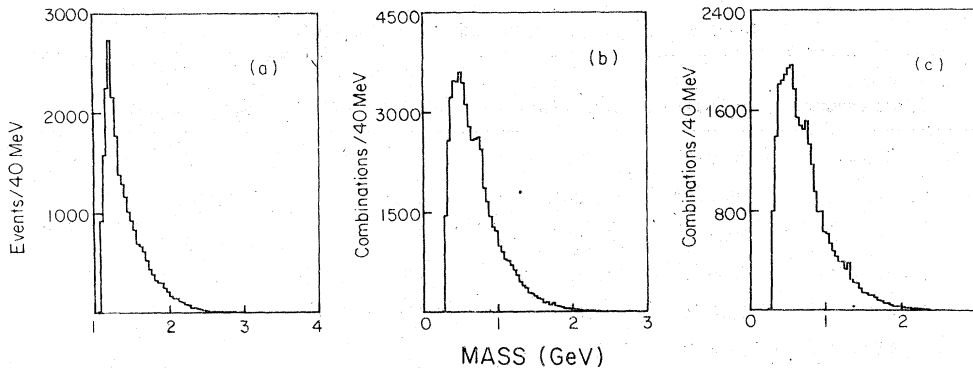


FIG. 10. Unfitted invariant-mass distributions for reactions (6) and (7): (a) $p\pi_s^+$ [reaction (6)]; (b) $\pi^+\pi^-$ [2 combinations/event; reaction (6)]; (c) $\pi^+\pi^-$ [3 combinations/event; reaction (7)].

nance formation.¹⁵ In fact at our level of statistics the reaction (5) final state is consistent with the assumption that it is produced entirely via one or more intermediate resonant states.

No previous study of the $n\pi^+\pi^+\pi^-\pi^-$ final state has reported the copious resonance production we observe.¹⁶⁻²¹ Some $\Delta^-(1232)$ production has been observed,¹⁷⁻²⁰ and slight indications of $\Delta^+(1232)$,¹⁹ ρ^0 ,^{19,20} and A_1 (Ref. 21) have been seen in different experiments. The failure of previous workers to clearly observe this behavior may, at least in part, be due to the difficulty of separating a clear sample of the $n\pi^+\pi^+\pi^-\pi^-$ final state from the background. This is a problem which we believe we have largely overcome.³

E. The reactions $\pi^+p \rightarrow \pi^+p\pi^+\pi^-MM$ and $\pi^+p \rightarrow \pi^+\pi^+\pi^-\pi^-MM$

Figures 9(a) and 9(b) display the missing-mass-squared (MM^2) distributions for reactions (6) and (7), respectively. The former distribution indicates significant η^0 production (i.e., the reaction $\pi^+p \rightarrow \pi^+p\pi^+\pi^-\eta^0$). To measure the cross section for η production we fitted this distribution to a Gaussian function for the η and a multi- π^0 production background.²² This fit yielded a cross section of $(397 \pm 43) \mu b$ for the reaction $\pi^+p \rightarrow \pi^+p\pi^+\pi^-\eta^0$ at 10.3 GeV/c.

The $p\pi_s^+$ invariant-mass distribution of reaction (6) [Fig. 10(a)] and the $\pi^+\pi^-$ invariant-mass distributions of reactions (6) and (7) [Figs. 10(b) and 10(c)] indicate significant $\Delta^{*+}(1232)$ and limited $\rho^0(770)$ production, respectively. However, owing to uncertainties in the background, no fits to these distributions were attempted. No hint of a $\Delta^{*+}(1232)$ signal was observed in the $p\pi_s^+$ invariant-mass distribution of reaction (6).

III. SUMMARY

We have given a comprehensive listing of the partial, total, and resonance production cross

sections for seven production channel resulting from the reactions $\pi^+p \rightarrow$ four-prong final states 10.3-GeV/c incident pion beam momentum. Of the seven channels studied, the final states $\pi^+p\pi^+\pi^-$, $\pi^+pK^+K^-$, and $n\pi^+\pi^+\pi^-\pi^-$ were found to be compatible with total production via quasi-n-body intermediate states. While this has been a well-known characteristic of the former final state for some time now, the same has not been so for the latter two. In fact, while a number of investigators have noted significant resonance production for the $\pi^+pK^+K^-$ final state, previous data regarding the $n\pi^+\pi^+\pi^-\pi^-$ final state have indicated a lack of any major resonance production.

ACKNOWLEDGMENTS

This experiment could not have taken place without the participation of a large number of people. We want to especially thank those physicists who took part in the early stages of the experiment and made important contributions to its progress: Gordon Charlton, Dave Crennell, Brian Deery, Dave Gilbert, Howard Gordon, K. W. Lai, and Suzanne Vallet. Equally important was the work of measuring, scanning, programing, and data handling. In particular we want to thank the following who contributed so much in these areas: Quais Ashraf, Bruce Bolin, Rodney Jones, Peter Kahan, Dave Kesterton, June Liu, Sheila Maggs, Dave McDonald, John Phillips, Alfred Sipprell, and the large band of measures and scanners at Toronto. We also express our appreciation to the POLLY group and all members of the SLAC staff who contributed to the success of the data acquisition.

This research was supported by funds from the National Research Council of Canada, administered by the Institute of Particle Physics.

*Present address: Physics Dept., Purdue University, Lafayette, Indiana 47907.

†Present address: Argonne National Laboratory, Argonne, Illinois 60439.

¹For a medium- or high-statistics bubble-chamber experiment the ionization estimates of tracks given by the automatic measuring machine play a predominant role in any hypothesis-selection algorithm. For details of how we optimized the conversion of the raw POLLY ionization data into an ionization χ^2 and probability for each hypothesis of an event see C. N. Kennedy, B. J. Deery, and A. W. Key, Nucl. Instrum. Methods **131**, 331 (1975).

²C. N. Kennedy, Ph.D. thesis, University of Toronto, 1976 (unpublished).

³C. N. Kennedy, A. W. Key, T.-S. Yoon, and P. D. Zemany, Nucl. Instrum. Methods **145**, 417 (1977).

⁴For a few of the many resonances we report, our level of statistical significance or our ignorance of the background makes our cross-section estimates unreliable. However, in cases where an enhancement corresponds to a well-established resonance, we nonetheless quote these values of cross section for the purposes of completeness.

⁵Particle Data Group, Rev. Mod. Phys., **48**, S1 (1976).

⁶The evidence for this enhancement in the present data is presented and discussed in Ref. 8. While there are three baryon resonances in this region postulated by phase-shift analyses [$\Delta(1890)$ ($J^P = \frac{5}{2}^+$), $\Delta(1910)$ ($J^P = \frac{1}{2}^+$), $\Delta(1950)$ ($J^P = \frac{7}{2}^+$)] the results of several previous investigations listed below indicate that this enhancement, observed in the 1.9-GeV region of the $p\pi^+$ invariant-mass distribution, is most likely identified with the $\Delta(1950)$. D. C. Colley *et al.*, Nucl. Phys. **B69**, 205 (1974); J. A. Gaidos and D. H. Miller; Phys. Rev. D **12**, 2565 (1975); S. U. Chung *et al.*, *ibid.* D **12**, 693 (1975).

⁷M. Aguilar-Benitez *et al.*, Phys. Rev. D **5**, 11 (1972).

⁸P. D. Zemany *et al.*, Nucl. Phys. B (to be published).

⁹J. W. Lamsa *et al.*, Nucl. Phys. **B41**, 388 (1972).

¹⁰This $K\bar{K}$ enhancement at 1.3 GeV is probably a com-

bination of f and A_2 meson production. Using the known branching ratios of the f and A_2 mesons and the f and A_2 cross sections given in Tables II and VI, respectively, we calculate that the $K\bar{K}$ enhancement cross section should be $15 \pm 3 \mu\text{b}$, in reasonable agreement with the measured value of $20 \pm 3 \mu\text{b}$ given in Table IV. Furthermore, we calculate that 66% of this cross section should be the result of f production. We tried fitting the $K\bar{K}$ enhancement first to anf , then to an A_2 , and finally to a combination of f and A_2 . The latter two fits gave very poor χ^2 values and we have thus quoted the fit to the f meson alone in Table IV.

¹¹Owing to the narrow width of the ϕ meson and our limited statistics, we did not perform a fit in the ϕ mass region.

¹²C. N. Kennedy, P. D. Zemany, and A. W. Key, Phys. Rev. D **16**, 2083 (1977).

¹³Our cuts for ω ($0.64 \text{ GeV} < m_{3\pi} < 0.84 \text{ GeV}$) and η ($m_{3\pi} < 0.64 \text{ GeV}$) production included the large bulk of these signals.

¹⁴J. H. Friedman, LRL Berkeley report, 1971 (unpublished).

¹⁵Our best estimate of this number is that the partial cross sections for resonance production account for $(86 \pm 10)\%$ of the total production cross section.

¹⁶M. Abolins *et al.*, Phys. Rev. Lett. **11**, 381 (1963); G. Goldhaber *et al.*, *ibid.* **12**, 336 (1964); F. E. James *et al.*, Phys. Rev. **142**, 896 (1966); C. Alff-Steinberger *et al.*, *ibid.* **145**, 1072 (1966); N. Armenise *et al.*, Nuovo Cimento **41A**, 159 (1966); P. Daronian *et al.*, *ibid.* **41A**, 503 (1966); M. Aderholz *et al.*, Nucl. Phys. **B8**, 45 (1968); C. C. Pöls *et al.*, *ibid.* **B25**, 109 (1970); J. W. Chapman *et al.*, Phys. Rev. D **3**, 39 (1971).

¹⁷S. Yamamoto *et al.*, Phys. Rev. **B140**, 730 (1965).

¹⁸E. E. Ronat *et al.*, Nucl. Phys. **B38**, 20 (1972).

¹⁹M. Aderholz *et al.*, Phys. Rev. **B138**, 897 (1965).

²⁰M. S. Alam *et al.*, Nucl. Phys. **B90**, 384 (1975).

²¹H. Grässler *et al.*, Nucl. Phys. **B75**, 1 (1974).

²²We assumed a combination of $2\pi^0$, $3\pi^0$, and $4\pi^0$ production for the background.